Available online at www.sciencedirect.com
SCIENCE DIRECT®
Physica E 19 (2003) 167–172
PHYSICA E
www.elsevier.com/locate/physe

Electron holographic characterization of nanoscale charge distributions for ultra shallow PN junctions in Si

P.S. Chakraborty[a,*], M.R. McCartney[b], J. Li[b], C. Gopalan[a], U. Singisetti[a], S.M. Goodnick[a], T.J. Thornton[a], M.N. Kozicki[a]

[a] *Center for Solid State Electronics Research, Arizona State University, Tempe, AZ 85287-6206, USA*
[b] *Center for Solid State Sciences, Arizona State University, Tempe, AZ 85287-1704, USA*

Abstract

This study extends electron holography as a quantitative characterization tool for nanoscale charge distributions associated with ultra shallow PN junctions in Si, which are needed for fabricating nanoscale MOSFETs, Si quantum dots and single electron transistors. The ultra shallow junctions were fabricated using rapid thermal diffusion from a heavily doped n-type surface source onto a heavily doped p-type substrate. Chemical characterization of the dopant profiles was performed using secondary ion mass spectrometry, which were analyzed to derive the metallurgical junction depth. 1-D characterization of the electrical junction depth associated with the electrically activated fraction of the incorporated dopants was performed using off-axis electron holography in a transmission electron microscope. 1-D potential profiles across the p–n junctions derived from electron holographic analysis were used to calculate the electric field and total charge distributions in the space charge region of the p–n junctions using numerical derivatives. Quantitative comparison between calculated electric field and total charge from the measured potential profiles and the simulated distributions using the secondary ion mass spectrometry profiles provide a reasonable estimate of the electrical activation of dopants in the ultra shallow junctions considered for this investigation.

Keywords: Electron holography; Ultra shallow junctions; Dopant activation; Rapid thermal diffusion; Space charge region

1. Introduction

The importance of having a 2-D method for mapping dopant and potential distributions in semiconductor devices has long been recognized [1]. The applicability and usefulness of off-axis electron holography as an electrical characterization tool for nanoscale charge distributions in ultra shallow PN junctions (USJs) in Si are examined here. These junctions are needed for fabricating nanoscale MOSFETs, quantum dots and single electron transistors in Si [2]. Recent investigations have demonstrated the capability of off-axis electron holography (EH) for mapping electrostatic potential in semiconductor devices with high sensitivity (0.1 V) and spatial resolution (~5–10 nm) [3–8].

Off-axis EH is a transmission electron microscope (TEM) technique that quantitatively measures the phase shifts of the electron wave front caused by the interactions with the electrostatic potentials of the

* Corresponding author. Tel.: +1-480-965-4097; fax: +1-480-965-3837.
E-mail address: partha.chakraborty@asu.edu (P.S. Chakraborty).

1386-9477/03/$ - see front matter © 2003 Published by Elsevier B.V.
doi:10.1016/S1386-9477(03)00302-3

specimen and thus allows the study of potential distributions associated with USJs in Si. The technique of EH is based on the interference of a high energy electron wave front scattered by a thin electron transparent sample with a coherent reference electron wave front, following which the interference pattern is reconstructed to derive the phase and amplitude information of the electron wave that was scattered by the thin sample. The reconstructed phase image of the electron wave that had passed through the specimen contains quantitative information about electrostatic potentials within the specimen. Digital processing of electron holograms has helped in developing a paradigm for quantitative EH [9–11].

In this investigation, off-axis EH is extended to quantify the 1-D electric field and total charge distributions in the space charge region (SCR) of the USJs and their electrical junction depth (EJD) using the potential profiles derived from the phase image in conjunction with Poisson's equation. The EJD is defined to be the depth from Si surface at which the maximum of the electric field occurs or the total charge density associated with the space charge region of the USJ goes to zero. These measured quantities are compared with the EJD, electric field and total charge distributions from simulations using SIMS profiles as shown in Fig. 1, as well as the metallurgical junction depth (MJD). The MJD is calculated to be the depth from Si surface at which the concentration of B atoms in the substrate is equal to the concentration of the phosphorus (P) atoms introduced by diffusion, both as measured by secondary ion mass spectrometry (SIMS) analysis. This comparison provides insight into the quantitative estimation of electrical activation of the incorporated dopants during the rapid thermal diffusion (RTD) process used to fabricate the USJs. Finally, an estimate of the lateral diffusion in one of the diffused junctions is also provided using EH.

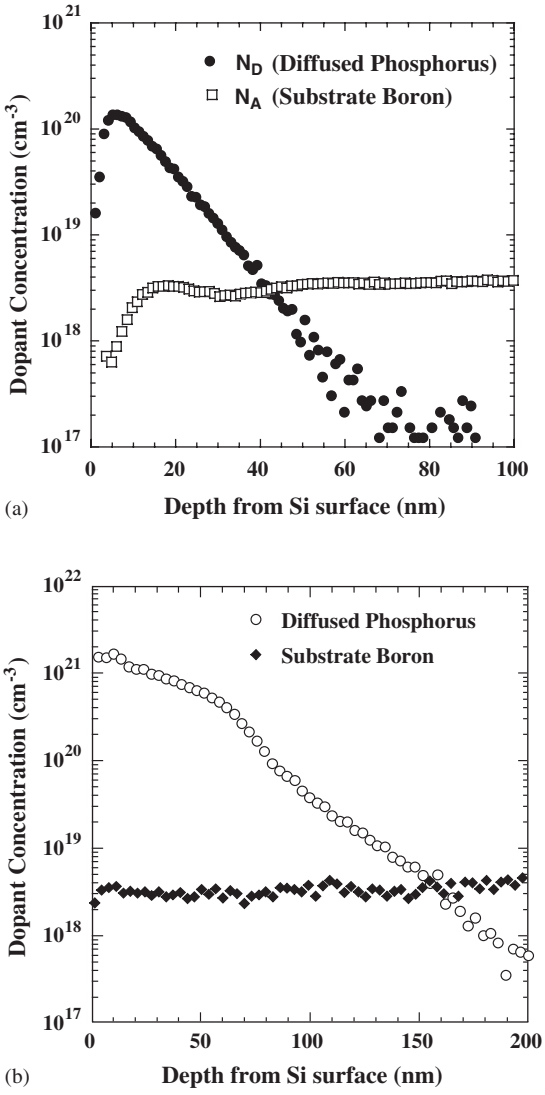

Fig. 1. SIMS profiles of dopants in the samples fabricated using RTD for electron holography. (a) USJ sample on which electron holographic analysis was done after an 850°C, 10 s RTD. (b) SIMS profile for the deep junction sample on which electron holographic analysis was done after 900°C, 60 s RTD.

2. Sample preparation

The ultra shallow n^+–p junctions used in this investigation were fabricated by RTD of P from a P-doped spin-on-glass (SOG) onto a p-type (1 0 0) Si substrate highly doped in the range 2.5×10^{18} to 6×10^{18} cm^{-3} with B. A Si substrate with ~2000 Å thick and patterned wet thermal SiO_2 meant to be a diffusion mask were used to prepare samples for electron holographic analysis. The P-doped SOG on the Si surface was treated with a RTD process, which forms an n^+–p ultra shallow junction (USJ) in the unmasked regions of Si.

An USJ sample fabricated using an 850°C 10 s RTD process, and a second sample with a deeper junction

fabricated using a RTD process at 900°C for 60 s, were used to prepare thin cross-sectional TEM specimens for electron holographic analysis. Henceforth, these samples will be referred to as the USJ sample and the deep junction (DJ) sample, respectively. SIMS analysis was done on a single die from each of the two samples in the unmasked diffusion window regions, after removal of the SOG with an HF solution.

TEM sample preparation was done in a similar way as detailed in a previous investigation [12]. A wedge-polishing technique was used in making the cross-sectional samples resulting in a 2° wedge in the specimens, which helps in correcting the thickness contribution to phase. Low angle, low energy Ar ion-milling was used to remove a large part of the thick SOG layer at the Si surface of the USJ wedge-shaped sample. The USJ sample was coated with a layer of amorphous carbon to avoid charging of the oxide and the SOG at the Si surface. The carbon-coating normally acts as a conducting path for the insulating surface layers, and also encapsulates any secondary electrons emitted from the sample, thus preventing charging of the sample.

The DJ wedge-shaped sample was not subjected to ion-milling and carbon-coating due to problems in sample preparation. This caused the cross-sectional sample to have more non-uniform thickness variation, which was evident in the 2D phase images. This sample showed evidence of charging due to the absence of a carbon-coating.

3. Experimental procedure

The samples were tilted away from the [1 1 0] zone axis to minimize diffraction [12]. The holograms were processed using Digital Micrograph scripting language [7]. The phase and the amplitude of the modulated wave were digitally reconstructed using Fourier analysis of the digitally recorded electron holograms. Thickness images of the sample were derived from reconstructed amplitude images assuming 85 nm as the inelastic mean-free-path (λ_i, IMFP) in Si [13]. This gives correct thickness only for the Si region of the sample since λ_i is unknown for the SOG or SiO_2.

1-D phase and thickness line scans were taken using lateral averaging from the 2-D phase and thickness images to improve the signal-to-noise ratio. A phase unwrapping algorithm was used to remove the modulo 2π phase wraps while deriving the 1-D phase line scans. The electron holographic studies for both the USJ and the DJ sample were performed using an acceleration voltage of 200 kV and an electrostatic biprism voltage of 140 V. A Lorentz minilens was used to optimize the field of view.

A 1-D Poisson solver program [14] was used to simulate the potential profile, electric field and total charge distributions associated with the P and B dopant distributions in Si, as measured by SIMS on the USJ samples. Partial activation from diffusion was accounted for by scaling down the diffused dopant profile by a constant factor.

4. Results and analysis

The SIMS analysis done on a part of the USJ sample is shown in Fig. 1(a). The large initial transient in the B profile in Fig. 1(a) is commonly seen when SIMS analysis of B is done using O_2^+ primary ions. A smaller transient is observed for the P profile as Cs^+ primary ions were used for P analysis, seen normally before a plateau in the Si signal is reached. The MJD observed in the USJ sample from the SIMS profiles of B and P in Fig. 1(a) is ~44 nm. The SIMS analysis done on a part of the DJ sample is shown in Fig. 1(b). The substrate B concentration is approximately 4×10^{18} cm^{-3} from the SIMS analysis on the DJ sample in Fig. 1(b). The MJD observed in the DJ sample from the SIMS profiles of B and P in Fig. 1(b) is ~165 nm.

The reconstructed phase images from part of the USJ sample and the DJ sample are shown in Figs. 2(a) and (b). The contrast appearing due to the brighter region in Si under the SOG in the diffusion window occurs due to formation of the junction by RTD of the dopant atoms from the SOG into the Si substrate. The brighter regions in Si indicate higher phase and hence higher electrostatic potential of the diffused n^+ region over the p-type Si substrate, indicating the existence of an n^+–p junction. As part of a previous investigation [12], analysis of the 1-D phase profiles for the USJ sample showed a phase enhancement in the diffused n^+ regions of the sample over the p-type substrate compared to the regions that were masked against diffusion.

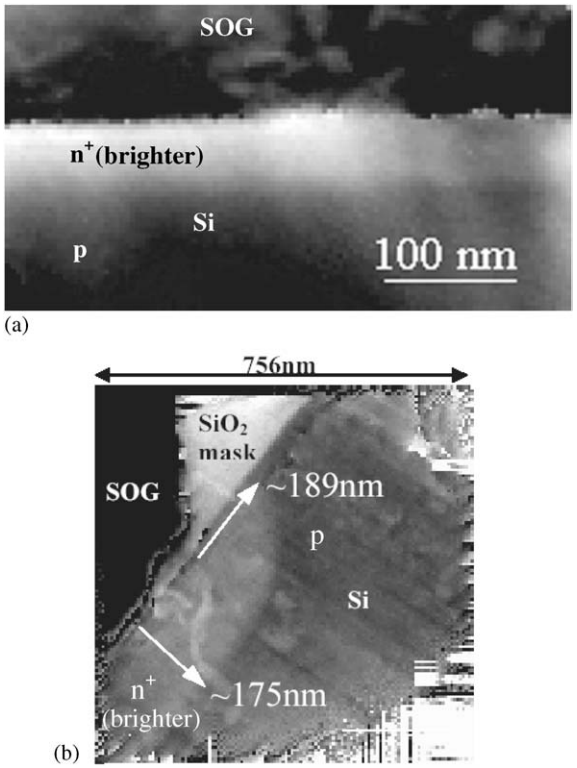

Fig. 2. (a) Phase image of a region of the USJ sample showing the bright region as a contrast due to the USJ formation. (b) Reconstructed phase image of the deep junction sample. The bright region in Si indicating the junction formation, while the bright region around the edge of the oxide diffusion mask indicates significant lateral diffusion under the oxide mask close to the diffusion window.

The phase images were scaled into potential maps using the following expression

$$V(x,y) = \frac{\phi(x,y)}{C_E t(x,y)} - V_0, \qquad (1)$$

where $\phi(x,y)$ is the phase shift relative to vacuum, C_E is an interaction constant depending on the acceleration voltage (0.00728 rad $V^{-1}nm^{-1}$ at 200 keV), and V_0 is taken as the mean inner potential of Si [15]. $V(x,y)$ and $t(x,y)$ are the 2-D potential and thickness mapping respectively across the sample. A previous investigation on the USJ sample reported the total potential variation from the Si surface to the substrate to be 1.2 V for the diffused junction corresponding to two line-scans (H3 and H6, not shown in Fig. 2(a)) in different regions of the sample, which is quite close to the bandgap of Si, as expected for these heavily doped junctions [12].

The electric field and total charge distributions associated with the SCR of the electrical junction are determined by successive differentiation of the 1-D potential profile obtained from the phase shift in Eq. (1). This numerical differentiation process is inherently noisy, particularly in the charge density, which is derived from the second order derivative as shown in Fig. 3(b). Fig. 3 shows the extracted electric field (a), and charge density (b), for the two different line-scans (H3 and H6) across the junction in the USJ sample. In comparison, the simulated electric field and charge density shown are calculated self-consistently using the measured SIMS profile of Fig. 1(a) as an input for the doping, and incomplete activation is taken care of by scaling down the diffused P profile appropriately by a constant factor (Figs. 3(a) and (b)). The maximum in the observed electric field in Fig. 3(a) can be taken as the EJD to avoid the ambiguity associated with its location from the noisy second derivative. The EJD derived for the USJ sample according to the above analysis of the 1-D potential profiles is found to be around ~42 to 44 nm for both line-scans H3 and H6 as shown in Fig. 3(a). This compares very closely with the metallurgical junction depth of ~44 nm for the USJ sample from Fig. 1(a). As shown in Figs. 3(a) and (b), better fits for the simulated quantities with their observed experimental values are obtained by assuming 70–80% activation of the diffused P atoms. This provides a reasonable quantitative estimate of the activation of incorporated dopants for the thermal budget used during the RTD process for fabricating the USJ sample.

Similar analysis to that performed on the USJ sample was also carried out on the electron holographic data from the deep junction (DJ) sample. Fig. 4(a) shows the total potential variation for the DJ sample into the substrate, while Fig. 4(b) shows the extracted electric field and charge density versus depth. The total potential drop from the surface to the substrate is ~1.25 V, which is somewhat higher than the Si band gap due to the degenerate doping of the n and p regions. The measured 1-D total charge distribution and field shown in Fig. 4(b) indicates an EJD of ~167 nm, which compares very closely with the MJD of ~165 nm derived from the SIMS profiles in Fig. 1(b), thus indicating the accuracy of the technique.

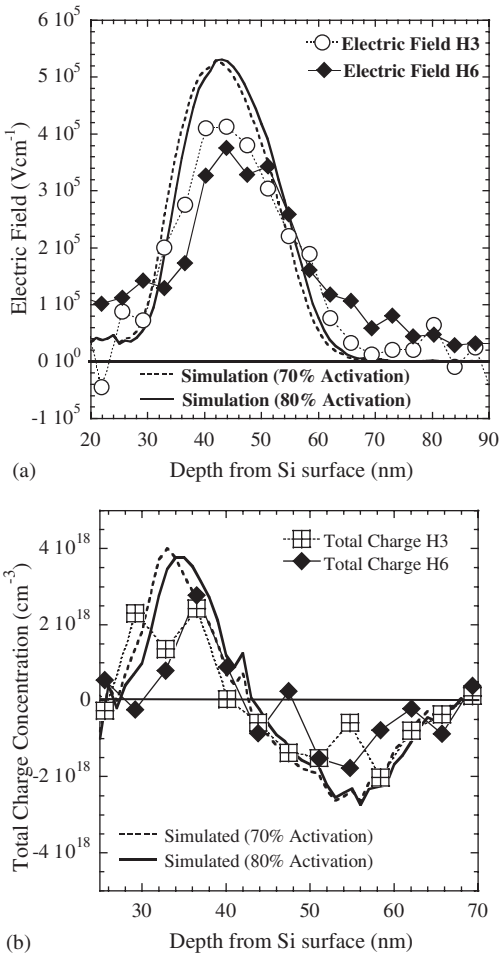

Fig. 3. (a) Comparison of the experimentally observed 1-D electric field distribution for the two potential line scans H3 and H6 with the simulated 1-D electric field distribution for the space charge region of the USJ sample for 70% and 80% activation. (b) Comparison of the experimentally observed 1-D total charge distribution for the two potential line scans H3 and H6 with the simulated 1-D total charge distribution for the space charge region of the USJ sample for 70% and 80% activation.

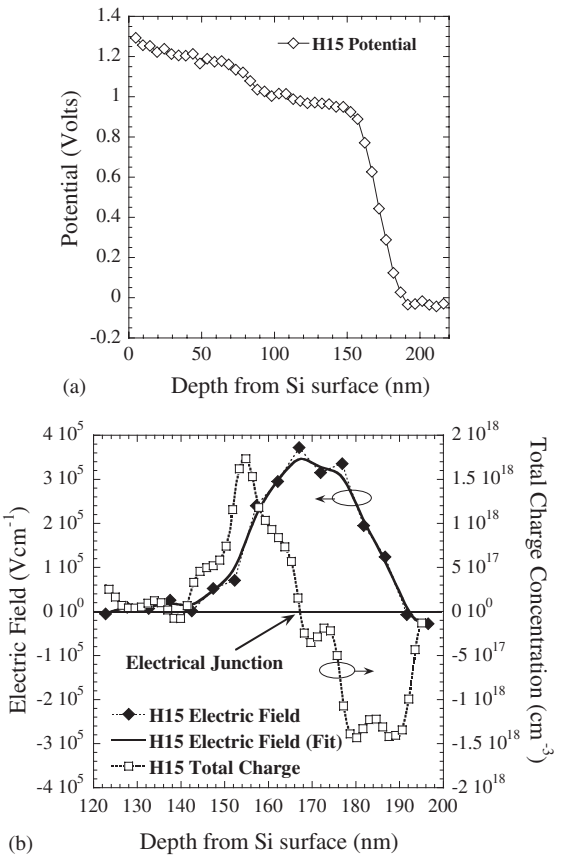

Fig. 4. (a) 1-D Potential profile calculated from the phase and thickness line scans corresponding to H15 in the region of the DJ. (b) 1-D electric field and total charge distributions calculated from the H15 potential profile gives a ~167 nm EJD.

The reconstructed phase image of a region of the DJ sample around the edge of the oxide mask shown in Fig. 2(b) does not indicate junction formation under the oxide far away from the edge of the mask. Fig. 2(b) indicates a junction formed by lateral diffusion under the oxide mask near the edge of the diffusion window. The distance over which the total potential variation occurs from lateral diffusion under the edge of the diffusion mask is observed to be ~189 nm, which is comparable to the vertical depth of ~175 nm over which the potential variation occurs under the diffusion window. This can be accounted for by the fact that the edge of the oxide diffusion mask is not vertical but gradual near the edge, leading to P diffusion through the thinner regions near the edge of the oxide mask into the Si substrate, leading to a higher lateral diffusion than what is expected under an abrupt edged diffusion mask. The phase image also indicates charging of the oxide, which leads to depletion of the Si under the oxide, indicated by a thin bright region.

The MJD based on the SIMS data is closely comparable to the experimentally measured EJD for the USJ sample as well as the DJ sample. The difference

in the MJD from the SIMS profiles and the experimental values of EJD can be accounted by the spatial resolution of the holographic data, which is limited to 5 nm in this analysis, and the depth resolution of the SIMS analysis.

5. Summary

This study has mainly focused on the SCR associated with the diffused USJs and extends the work from a previous investigation [12]. In this study, off-axis electron holography has been used for quantitative analysis of USJs. 1-D potential profiles derived from off-axis electron holograms have been analyzed to measure the EJD for both the USJ sample and the DJ sample. This analysis also led to the estimate of activation for the USJ sample and lateral diffusion in the DJ sample. The numerical derivative (ND) method for extracting the electric field and total charge profiles in the space charge region of a p–n junction provides a simple and reasonably accurate tool even when higher order derivatives gets noisier. The ND method here has been applied to both the USJ and the DJ sample and has been shown to resolve junction depths in the range from ~40 nm to ~170 nm. On the other hand, this ND method for resolving electrical junction depths using electron holographic data leads to a reduced accuracy in the magnitude of the experimentally observed quantities relative to their spatial location. A key to higher accuracy in the magnitude of the derived measurements is through achievement of more uniformity in sample thickness and reduction of noise in the phase measurements. Higher accuracy in the spatial resolution of such measurements is possible through use of a higher resolution CCD camera in recording the holograms.

Acknowledgements

This work was supported by the Office of Naval Research MURI program and by Semiconductor Research Corporation under the grant SRC#942.001. The authors would like to thank the Center for High Resolution Electron Microscopy and K. Franzreb of the SIMS facility at Arizona State University for assistance.

References

[1] A.C. Diebold, M.R. Kump, J.J. Kopanski, D.G. Seller, J. Vac. Sci. Technol. B 14 (1) (1996) 196.
[2] International Technology Roadmap for Semiconductors, Semiconductor Industry Association, San Jose, CA, 2001, Online available: http://public.itrs.net/Files/2001ITRS/.
[3] M.R. McCartney, D.J. Smith, R. Hull, J.C. Bean, E. Völkl, B. Frost, Appl. Phys. Lett. 65 (20) (1994) 2603.
[4] W.D. Rau, F.H. Baumann, HH. Vuong, B. Heinemann, W. Höppner, C.S. Rafferty, H. Rücker, P. Schwander, A. Ourmazd, IEDM Tech. Dig. (1998) 713.
[5] W.D. Rau, P. Schwander, F.H. Baumann, W. Höppner, A. Ourmazd, Phys. Rev. Lett. 82 (12) (1999) 2614.
[6] M.A. Gribelyuk, M.R. McCartney, J. Li, C.S. Murthy, P. Ronsheim, B. Doris, J.S. McMurray, S. Hegde, D.J. Smith, Phys. Rev. Lett. 89 (2) (2002) 025502(1–4).
[7] M.R. McCartney, M.A. Gribelyuk, J. Li, P. Ronsheim, J.S. McMurray, D.J. Smith, Appl. Phys. Lett. 80 (17) (2002) 3213.
[8] A.C. Twichett, R.E. Dunin-Borkowski, P.A. Midgley, Phys. Rev. Lett. 88 (23) (2002) 238302(1–4).
[9] L. Reimer, Transmission Electron Microscopy, Springer, Berlin, 1989.
[10] A. Tonomura, L.F. Allard, G. Pozzi, D.C. Joy, Y.A. Ono (Eds.), Electron Holography, North-Holland/Elsevier, Amsterdam, 1995.
[11] E. Völkl, L.F. Allard, D.C. Joy (Eds.), Introduction to Electron Holography, Kluwer Academic/Plenum Publishers, Dordrecht/New York, 1998.
[12] P.S. Chakraborty, M.R. McCartney, J. Li, C. Gopalan, M. Gilbert, S.M. Goodnick, T.J. Thornton, M.N. Kozicki, IEEE Trans. Nanotechnol. 2 (2) (2003).
[13] M.R. McCartney, M. Gajdardziska-Josifovska, Ultramicroscopy 53 (1994) 283.
[14] I.-H. Tan, G.L. Snider, L.D. Chang, E.L. Hu, J. Appl. Phys. 68 (8) (1990) 4071, Online available: http://www.nd.edu/~gsnider/.
[15] M. Gajdardziska-Josifovska, M.R. McCartney, W.J. de Ruijter, D.J. Smith, J.K. Weiss, J.M. Zuo, Ultramicroscopy 50 (1993) 285.